mmChoir: Exploiting Joint Transmissions for Reliable 60GHz mmWave WLANs

Ding Zhang
Computer Science Department
George Mason University
Fairfax, VA, USA
dzhang13@gmu.edu

Mihir Garude
Computer Science Department
George Mason University
Fairfax, VA, USA
mgarude@gmu.edu

Parth H. Pathak
Computer Science Department
George Mason University
Fairfax, VA, USA
phpathak@gmu.edu

ABSTRACT

60 GHz millimeter-wave WLANs are gaining traction with their ability to provide multi-gigabit per second data rates. In spite of their potential, link outages due to human body blockage remain a challenging outstanding problem. In this work, we propose mmChoir, a novel proactive blockage mitigation technique that utilizes joint transmissions from multiple Access Points (APs) to provide blockage resilience to clients. We derive a new reliability metric based on angular spread of incoming paths to a client and their blockage probabilities. The metric can be used to intelligently select joint transmissions that can provide higher reliability. The reliability metric along with a novel interference estimation model, is used by mmChoir's scheduler to judiciously schedule joint transmissions, and increase network capacity and reliability. Our testbed and trace-driven simulations show that mmChoir can outperform existing beamswitching based blockage mitigation scheme with on an average 58% higher network throughput.

CCS CONCEPTS

• **Networks → Mobile networks**; **Wireless local area networks**;

KEYWORDS

60 GHz WLANs, Millimeter-wave wireless networks, Joint transmissions, Interference management

1 INTRODUCTION

60 GHz millimeter-wave networks have emerged as a viable candidate for designing the next generation of WLANs. With the development of standards like IEEE 802.11ad [7] and 802.11ay [6], these networks can provide multi-gigabit per second data rates supporting applications like augmented/virtual reality, ultra high definition video streaming, sync-and-go, etc. In order to compensate for the higher path loss experienced at 60 GHz frequencies, directional antennas such as phased antenna arrays are employed to beam the signal in a desired direction. In spite of their great potential, outages due to link blockage remain one of the most important outstanding problems in reliable link layer connectivity in 60 GHz WLANs. Human body blockage of a mmWave link results in a loss of 20 to 30 dB [19], resulting in a disconnection of two endpoints.

Researchers have proposed a variety of solutions [5, 20, 26] which primarily rely on beam switching where an alternate (possibly reflected) path is used to recover the link blockage. However, these approaches have three important limitations: (1) They are inherently reactive in nature where the blockage recovery is only initiated after the link is blocked. This has led to investigation of proactive switching schemes [23, 26] but these schemes rely on motion sensor information from mobile devices to determine pose, orientation, heading, etc. (2) Although some existing techniques intelligently detect blockages (beam correlation [20] or probing [5]), beamswitching can yield limited benefits when the blockage occurs close to the transmitter or receiver. In fact, such blockages are more likely in WLAN scenarios where user's body blocks the signal from AP to her mobile device (also referred as self-body blockage). (3) Existing beamswitching-based schemes are primarily studied for single isolated point-to-point link scenarios. However, as we move towards 60 GHz enterprise WLANs, more complex scenarios with multiple APs, interfering links and paths have to considered and relevant challenges should be addressed.

In this paper, we present a proactive blockage mitigation technique for 60 GHz WLANs. With the emergence of dense millimeter-wave wireless networks [13], larger indoor spaces are likely to be covered using multiple APs in 60 GHz WLANs with more overlap of their coverage area. The deeper overlap between the cells of multiple APs can be exploited to enable Coordinated Multi-Point (CoMP) Joint Transmissions (JT) where two or more APs jointly transmit to a client. We show that the coordinated joint transmissions from APs to a client can substantially improve the blockage mitigation performance. The presence of additional AP(s) creates spatial diversity when their paths towards a client are sufficiently separated in terms of Angle-of-Arrival (AoA). Based on these observations, we design a new blockage mitigation technique, mmChoir, that judiciously chooses which APs participate in a JT to a client depending on the angular separation of their paths to the client and their blockage probability. mmChoir can intelligently adapt the number of joint transmissions depending on the blockages and can carefully balance the spatial reuse to achieve high throughput along with reliability. Since mmChoir relies on multiple, spatially diverse paths to transmit data to a client, it also provides robustness against self-body blockages.

Challenges and Contributions: To fully realize the potential of JTs, we address the following challenges:

(1) JT Selection: The strength of joint transmissions in combating blockages is dependent on the selection of APs and the paths

Mobihoc '18, June 26–29, 2018, Los Angeles, CA, USA

ACM ISBN 978-1-4503-5770-8/18/06…$15.00
https://doi.org/10.1145/3209582.3209608

they use to communicate with a client. Paths which provide higher angular separation are less likely to be affected concurrently by a blockage. However, this requires carefully quantifying the spatial diversity.

We propose a novel metric (referred as reliability score) that captures the level of spatial diversity provided by JTs. The metric is based on angular spread of AoA for multi-path channel adapted for multi-level codebook-based beamforming. The reliability score uses the Power Angular Profile (PAP) from the beamforming phase and the blockage probability of component paths to provide an effective way of evaluating the quality of JTs.

(2) Interference Estimation: Employing joint transmissions can improve the reliability but may increase the interference footprint due to multiple paths transmitting together. Also, capturing interference relationships between paths (individual as well as JTs) can require prohibitively large number of measurements.

In order to estimate the interference relationship between the links, we develop an interference model (analogous to the protocol interference model) which can efficiently construct an interference conflict matrix. The estimation process does not require any measurements other than the beamforming training which is already used by APs and clients in existing 802.11ad MAC protocol. The model can also estimate the interference for joint transmissions and can account for the receiver beamwidth dilation needed in certain JTs.

(3) Blockage and interference aware scheduling: The interplay between blockage tolerance and spatial reuse in presence of JTs requires judiciously scheduling the links such that the link layer robustness is improved through coordination while the detrimental effects of increased interference do not produce serious penalties in terms of network capacity.

Based on the reliability score and spatial reuse score, we propose a centralized, blockage and interference-aware scheduling algorithm that aims at increasing the reliability as well as the spatial reuse. The proposed scheduler adapts to the level of blockage to intelligently adjust the level of coordination (number of JTs used and number of APs involved in each JT) needed for higher reliability and network capacity.

(4) Trace-driven Simulations: We evaluate mmChoir using our 60 GHz testbed and simulations in three different types of rooms and varying levels of human blockages. It is observed that in case of higher blockages, mmChoir significantly outperforms the existing scheme which does not use joint transmissions, while in case of fewer blockages, it adapts to reduce the amount of joint transmissions and maintains a comparable performance. We find that mmChoir achieves on an average 58% increase in network throughput under high blockage scenarios compared to a beam-switching based blockage mitigation scheme. Also, when utilizing JTs, coordination between 2 APs is often sufficient to provide the blockage resilience.

The remaining paper is organized as follows. Section 2 provides motivation and mmChoir overview. Section 3 discusses reliability score and Section 4 outlines the interference estimation process. Section 5 discusses our blockage and interference aware scheduler and we evaluate mmChoir in Section 6. We discuss related work in Section 7 and conclude in Section 8.

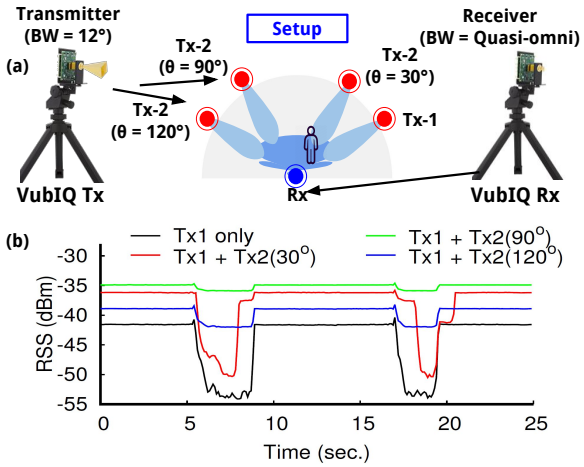

Figure 1: (a) 60 GHz software radio and horn antenna setup (b) Tx-1 and Tx-2 with larger angular separation provides higher robustness to blockages

2 MOTIVATION AND APPROACH

2.1 Motivation

We first study blockage and its effect on link layer performace using our software-radio testbed to demonstrate how joint transmissions can help in relieving the performance degradation. In the experiment setup (Fig. 1a), we use a software-radio 60 GHz testbed where the transmitter and receiver are composed of USRP [21] software radio as baseband processor, VubIQ 60 GHz RF frontend [22] and a horn antenna. The receiver uses quasi-omni antenna pattern and Tx-1 is located at a fixed angle as shown in Fig. 1a. Another Tx (Tx-2) sends data to the Rx along with the Tx-1. We vary the angle between Tx-1 and Tx-2 while a human is walking closer to the Rx, creating blockage events. Fig. 1b shows the total RSS at the Rx for four location combinations. We observe that when only Tx-1 is used, a blockage event results in 12dB loss. When Tx-2 is added at 30° angular separation, the overall RSS increases, but due to smaller angular separation, the blockage-related loss does not improve significantly. However, further increasing the angular separation (90° and 120°), the RSS loss significantly drops. This is because signal arriving from wider angles are less likely to be blocked by the same blockage. If we can use joint transmissions from multiple, spatially diverse APs to send signal to a client, it can provide added robustness against the blockages. We note that when the angular separation is 120°, the non-blockage RSS decreases because wider angle does not fully leverage the directional receiver gain. This means that while choosing the JTs, it is also necessary that the receiver's beamwidth is carefully adapted to fully exploit the spatial diversity.

2.2 System Overview

We now provide an overview of codebook-based beamforming used by mmChoir and then provide a system overview.

Multi-level Codebook: Due to the formidable complexity of optimal beamforming, 60 GHz devices rely on a predefined set of

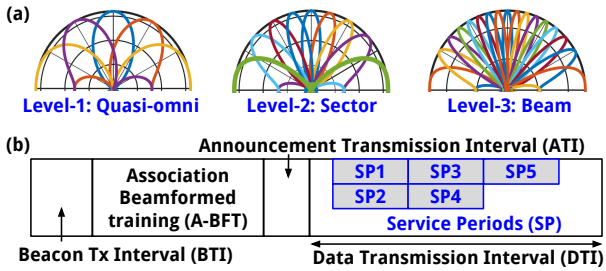

Figure 2: (a) Multi-level codebook with quasi-omni, sector and beam patterns, (b) 802.11ad Beacon Interval (BI) including time-divided service periods

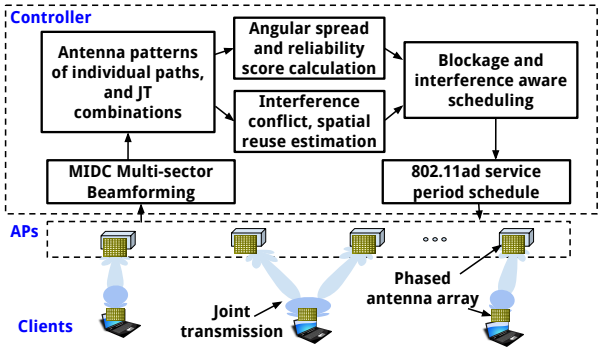

Figure 3: mmChoir **overview**

beamforming weights referred as a codebook. A codebook is a $A \times P$ matrix where A is the number of antenna elements in the array and P is the number of beamforming weight vectors (also known as patterns). In this work, we use DFT-based codebook design [9] which is proven to achieve a uniform gain in all directions. The DFT codebook matrix is calculated using

$$w(a,p) = \frac{1}{\sqrt{A}} e^{-j2\pi(a-1)(p-1)/P} \quad (1)$$

where $a \in \{1, ..., A\}$ and $p \in \{1, ..., P\}$. We use a multilevel codebook technique (used in [5, 26]) which generates three different levels of beamwidths referred as quasi-omni, sectors and beams. The 2-dimensional radiation patterns of the three levels are shown in Fig. 2(a).

Multi-AP Multi-sector Beamforming: IEEE 802.11ad beamforming training (BFT) procedure searches the codebook beams to find the maximum signal strength of Tx and Rx beam pairs. The BFT process is carried out in a dedicated time period within the 802.11ad beacon interval as shown in Fig. 2 (b). With joint transmissions, it is necessary that a client trains and determines its receiving beam with each AP available in its range. Additionally, mmChoir does not simply rely on the strongest path (typically LOS) between an AP and a client, but also determines other sub-optimal beam pairs (possibly over reflected paths). mmChoir uses an optional procedure referred as Multiple Sector ID Capture (MIDC)[7] in 802.11ad protocol to search for multiple pairs of beams (different paths) that Tx and Rx can use for communication.

Our proposed framework of joint transmissions is designed to operate within the 802.11ad MAC protocol. The 802.11ad utilizes a hybrid MAC protocol which includes time-divided dedicated Service Periods (SP) and Contention based Access Periods (CBAP). In this work, we primarily focus on dedicated SPs where one or more APs can transmit to a client in any given SP (as shown in Fig. 2(b)). Note that multiple SPs can be scheduled together in case of spatial reuse. mmChoir is a centralized system where a *controller* connected with the APs dictates the scheduling and joint transmissions (shown in Fig. 3). We only focus on *downlink traffic* and scheduling of individual or joint transmissions from APs to clients. The joint transmissions require that the APs and controller are connected through a high-bandwidth, low-latency *WLAN backhaul* (often referred as ideal backhaul in cellular networks [10]). This can be made possible through high-speed wired connections (e.g., fiber optics).

mmChoir Overview: Fig. 3 shows different modules of the mmChoir. The controller asks the APs to perform MIDC procedure with clients to determine multiple paths [1] between them. This path set is then used by the controller to calculate feasible joint transmission combinations. The set of path (individual and joint transmission) and their beam patterns are then used to calculate the angular spread and combined with blockage probabilities to derive a *reliability score*. The reliability score of a path quantifies how much robustness it can provide in presence of blockage(s). The path set is also used by the controller to assess the interference relationships (as a conflict matrix) between the paths and the allowable *spatial reuse*. The reliability and spatial reuse scores are input to the scheduling algorithm which determines a blockage and interference-aware schedule. The schedule is then distributed to the APs in the form of 802.11ad time-divided service periods.

3 RELIABILITY OF JTS

After determining multiple paths between each AP and client, we are now interested in finding which path can be used jointly to carry out joint transmissions from multiple APs to a client and how reliable such joint transmissions are.

The output of the multi-AP, multi-sector beamforming is a set S of candidate paths $s_i = \{Tx_i, Tx_i^p, Rx_i, Rx_i^p, rss_i\}$ where Tx_i is a transmitter (e.g., AP) using its beam pattern Tx_i^p to communicate with a receiver (e.g., client) Rx_i which is using its beam pattern Rx_i^p and rss_i is the received signal strength for that path. In mmChoir, all possible combinations of single paths is considered as joint transmissions. If the number of clients is n, the average number of APs in the range of a client is $m'(m' \leq m$ where m is the total number of APs), and average number of paths between a client and an AP is k, the average number of individual paths is $n \times m' \times k$. Let Q be the maximum number of APs that can be involved in a joint transmission, the total number of single and joint paths in S can be calculated as $|S| = n \times \left(\sum_{i=1}^{Q} \binom{m'}{i} k^i\right)$. In practice, Q is likely to be small due to the limited number of APs in a client's range and given that 60 GHz mmWave channels are sparse, $k \leq 5$ [19, 24]. Hence, the number of joint transmission combinations are likely to be limited in practical scenarios.

[1] We refer to a link layer connection as a link, while a path means a propagation path. A link can be scheduled over an individual path or a joint transmission paths (combination of individual paths).

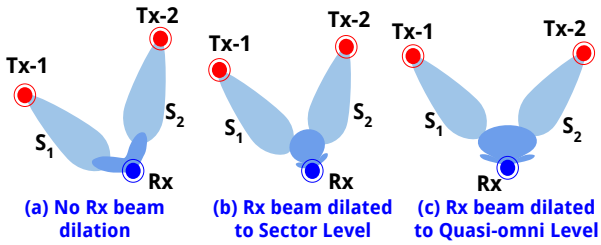

Figure 4: Receiver beamwidth adaptation for JTs

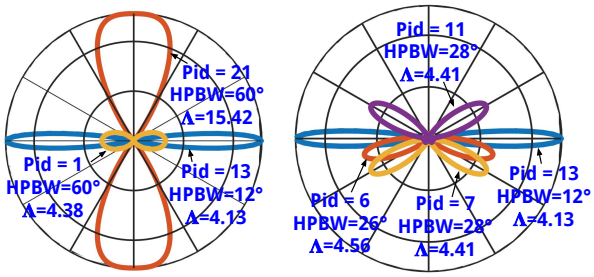

Figure 5: Angular spread (Λ) of different antenna patterns: Λ is higher for patterns with spatially diverse AoAs, higher gain and wider beamwidths

3.1 Receiver Beamwidth Adaptation

Our first challenge in utilizing the joint transmissions is to address the deafness problem at the receiver. Since a joint transmission is a combination of single paths, the transmit beam patterns on each AP involved in the JT can remain unchanged, however, the receiver beam pattern needs to be adapted. This is shown in Fig. 4. Adapting the receiver's beam pattern allows it to receive data from multiple APs simultaneously. Let s' be a joint transmission over individual paths s_1 and s_2 as shown in Fig. 4.

Case 1: Unchanged receiver pattern: If the receiver beam patterns of the individual single paths of a JT are the same, then the JT also uses the same receiver beam pattern. This is shown in Fig. 4a.

Case 2: Receiver beamwidth dilation: If the receiver beam patterns of the individual paths of a JT are not the same, then the receiver uses a dilated beam pattern for JT. The dilated beam pattern is chosen from the multi-level codebook (discussed in Section 2) such that it includes all the beam patterns of the individual paths. Note that depending on the individual paths, the wider beam pattern can be a sector (Fig. 4b) or even quasi-omni (Fig. 4c). In order to maintain higher gain, mmChoir dilates the beam to the next upper level (sector or quasi-omni) necessary to cover the beam patterns (Fig. 2a).

Note that the RSS of individual transmissions is determined during the beam-searching process. However, measuring the RSS of each possible combination of joint transmission is impractical due to its very high time overhead. This requires that the RSS of the joint transmission path is estimated from the individual paths. If a joint transmission path s' is composed of $s_1 = \{Tx_1, Tx_1^p, Rx_1, Rx_1^p, rss_1\}$ and $s_2 = \{Tx_2, Tx_2^p, Rx_2, Rx_2^p, rss_2\}$ and uses an adapted receiver pattern $Rx_i^{p'}$, then the RSS of s' can be estimated as $rss_1 + rss_2 - \mathbb{G}(Rx_1^p) - \mathbb{G}(Rx_2^p) + \mathbb{G}(Rx_i^{p'})$ where $\mathbb{G}()$ is the gain of the antenna pattern.

3.2 Reliability Metric

Second challenge in using JTs is that it is necessary to quantify the reliability of the incoming paths for a client using a metric. In this section, we propose a metric *(reliability score)* which combines (1) the angular spread of receiver antenna pattern (beamwidth and gain in different directions) and (2) blockage probability of paths involved in a JT. The metric can then be used to compare different joint transmissions in terms of their robustness to blockages and their RSS.

Angular Spread: A metric referred as *Angular spread* was proposed in [24] to model the Angle-of-Arrivals (AoA) of a multi-path channel at the receiver. We leverage the angular spread metric to model the spatial diversity of joint transmissions. Specifically, we use a non-normalized version of angular spread adapted for the codebook-based receiver patterns. Let $\mathbb{G}(Rx_i^p(\theta))$ be the angular gain profile of a receiver (Rx_i) for its pattern Rx_i^p. Assuming a unit power from all directions, the Power Angular Profile (PAP) of the pattern can be calculated as $\mathbb{P}(Rx_i^p(\theta)) = \mathbb{G}(Rx_i^p(\theta))$. Let F_n be the n^{th} fourier transform of $\mathbb{P}(Rx_i^p(\theta))$ defined as

$$F_n = \int_0^{2\pi} \mathbb{P}(Rx_i^p(\theta))\, e^{jn\theta}\, d\theta \tag{2}$$

and our revised angular spread metric (Λ) is calculated as

$$\Lambda(Rx_i^p) = \sqrt{\|F_0\|^2 - \|F_1\|^2} \tag{3}$$

In case of JTs, $\mathbb{P}(Rx_i^p(\theta))$ is calculated for receiving antenna pattern Rx_i^p after the beamwidth adaptation.

The proposed metric Λ achieves a higher value for receiving patterns that have *(i) wider separation between AoAs, (ii) higher gain and (iii) wider beamwidths.* Fig. 5 shows Λ of different antenna patterns that can be used for a JT. It can be observed that Patterns 1 and 21 have the same beamwidth but Pattern 21 has higher Λ due to its higher gain and receiving power. Hence, a joint transmission using Pattern 21 is likely to have higher reliability. Λ of Pattern 6 is higher than that of Pattern 7 due to wider angular separation between the main lobes. Patterns 13 and 21 have the same gain, however, Pattern 21 has wider beamwidth which substantially increases its Λ as wider beamwidths provide much higher resistance to blockages.

Reliability Score: We now use the angular spread (Λ) to calculate a reliability score for each path in S (including individual path and joint transmissions). Let s' be a joint transmission composed of individual paths $\{s_1, s_2, ..., s_R\}$ with adapted receiver beam pattern Rx_i^p. If $P_b(s_r)$ is the blockage probability of the individual path s_r, then the probability that at least one path in s' is not blocked can be calculated as $1 - \prod_{r=1}^{R} P_b(s_r)$. This probability of successful transmission for the JT is combined with its angular spread to calculate the reliability score δ as follows

$$\delta(s') = \Lambda(Rx_i^p) \times \left(1 - \prod_{r=1}^{R} P_b(s_r)\right) \tag{4}$$

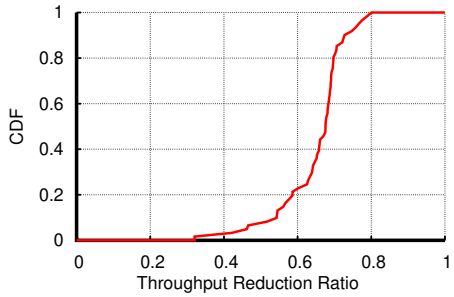

Figure 6: Non-uniform codebook patterns and wide beamwidths can result in non-trivial interference between 60 GHz WLAN links

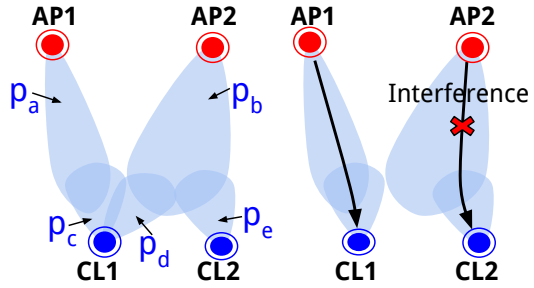

Figure 7: Two path AP1-CL1 and AP2-CL2 interfere with each other due to overlap in receiving patterns (p_c and p_d) at CL1

The blockage probability of individual paths is dependent on the characteristics of indoor mobility and difficult to be known in advance. Hence, mmChoir uses a feedback based adaptive scheme where after each time slot, the fraction of frames lost due to blockage on a path is used to update the blockage probability of that path. The updated probabilities are used to calculate the new reliability scores in the next time slot. The updated reliability scores enable mmChoir to proactively provision robust transmissions in the next time slot as we will discuss in Section 5.

4 INTERFERENCE ESTIMATION WITH JT

We firstly evaluate the impact of the interference on 60 GHz link throughput. Here, the total throughput of two links using Netgear 802.11ad routers and Acer laptops with 60GHz chipset (QCA9500 [11]) are measured separately and concurrently at 70 different location combinations in a laboratory. The throughput reduction ratio is calculated as $\frac{I_{wo}-I_w}{I_{wo}}$ where I_{wo} and I_w are sum of throughput for two links without and with interference respectively. CDF of the measured ratio is shown in Fig. 6. It can be observed that although 60 GHz mmWave link transmissions are directional, non-trivial sidelobes, non-uniform antenna patterns and wider beamwidths [15, 17, 23] can result in substantial interference between the links. Measuring the interference between each pair of links is prohibitively expensive [8], especially in our case where the links also include joint transmissions. Instead, mmChoir relies on a conservative estimation of interference derived from the set of paths (S) and the beam patterns used by APs and clients in each path.

Interference Model: We observe that the interference relationships between different paths are primarily dependent on the antenna patterns used by the transmitter and receiver. Through the multi-AP, multi-sector beamforming process, the Tx and Rx beam pattern information is available at the controller for all APs and clients, and their multiple paths. mmChoir leverages this information for inferring interference relationships between paths. We use a conflict matrix ($|S| \times |S|$) to represent the interference relationship between different paths in S (individual as well as joint transmissions). We now describe three rules that is used by mmChoir along with the beamforming information to build the conflict matrix. The rules are first explained in terms of individual transmissions and then we discuss how they can be generalized for joint transmissions.

(1) Transmit conflict: One transmitter cannot transmit to multiple receivers at the same time. In the context of mmChoir, this means that an AP cannot transmit to multiple clients at the same time. In this work, we do not consider the Multi-User MIMO scenario. Formally, a transmission path $s_i = \{Tx_i, Tx_i^p, Rx_i, Rx_i^p, rss_i\}$ interferes with $s_k \in S$ where $s_i \rightarrow Tx_i = s_k \rightarrow Tx_k$.

(2) Receive Conflict: Unless it is a joint transmission, two transmitters cannot send different data to the same receiver at the same time. This means that unless jointly transmitting, two APs cannot send different data to a client at the same time. Formally, an individual path s_i interferes with all other individual paths s_k where $s_i \rightarrow Rx_i = s_k \rightarrow Rx_k$.

(3) Interference Conflict: For a transmission path s_i, let P_r be a set of patterns that overlap with Rx_i^p, $S_R \subset S$ be a subset of paths to Rx_i which use a pattern $p \in P_r$ as its receiving pattern, then every path in $s_j \in S_R$ interferes with s_i. Also, let P_t be a set of transmit patterns used in the set of paths S_R, and S_T be a subset of paths which use a pattern $p \in P_t$ as its transmit pattern, then every path in $s_j \in S_T$ interferes with s_i.

Fig. 7 shows an example scenario to demonstrate interference conflict. Here, there are three transmission paths $s_1 = \{AP_1, P_a, CL_1, P_c, rss_1\}$, $s_2 = \{AP_2, P_b, CL_1, P_d, rss_2\}$, and $s_3 = \{AP_2, P_b, CL_2, P_e, rss_3\}$. We note that s_1 interferes with both s_2 and s_3. As per the above mentioned Rule 3, receiving patterns P_c and P_d overlap with each other. This means that path s_2 which has P_d as its receiving pattern interferes with s_1. Also, all paths which use the transmit patterns P_b also interfere with s_1. This is because when s_1 is active, if AP_2 transmits using P_b, there can be non-trivial interference at CL_1 due to overlap between P_c and P_d.

Interference with JTs: The above mentioned rules can also be used for capturing interference in case of joint transmissions. Rule 1 applies directly and while in terms of Rule 2, two joint transmissions or one joint transmission and one individual transmission, both of which have the same receiver cannot be scheduled at the same time. While determining the interference for a joint transmission path, Rule 3 needs to be applied to each individual path of the joint transmission to determine the interfering paths for that joint transmission.

The above mentioned interference model is analogous to widely used *protocol interference model* [1, 4]. There are two salient advantages of the model. First, it only relies on information available from beamforming phase and require no additional measurements. Second, it can operate on any codebook and its beam patterns as it only requires knowing the angular profile of the beam patterns.

This means that even when the patterns exhibit irregularities, no changes to the above mentioned rules are needed. The model can be combined with SINR measurements to develop a physical interference model, however, we leave that to future work.

Spatial Reuse Score: The conflict matrix C is generated at the controller by traversing through each path $s_i \in S$ (individual as well as joint transmission) and checking the above mentioned rules. Interference between two paths s_i and s_j is indicated as $C[s_i][s_j] = 1$ and 0 otherwise. We note that the process needs to be performed only in case of changes in S. Based on the conflict matrix, a spatial reuse score is calculated for each transmission path in S. The spatial reuse score β of a transmission path s_i is calculated as $\beta(s_i) = 1 - \left(\sum_{j=1}^{|S|} C[s_i][s_j]\right) / (|S|)$. The spatial reuse score of a path is a ratio of number of other paths it can be scheduled with to total number of paths in the network.

5 MMCHOIR SCHEDULER

We now present a scheduling algorithm that utilizes the reliability and spatial reuse metrics to create a blockage and interference aware schedule. The problem of scheduling wireless links can be modeled as problem of finding maximum independent set in a conflict graph. Given the problem is NP-hard, many heuristic-based algorithms are proposed [2, 14].

Blockage and Interference-aware Scheduling: In case of mmChoir, both reliability and spatial reuse directly affect the achievable network throughput. We note that there are obvious trade-offs between the robustness and spatial reusability of links. A joint transmission composed of multiple spatially diverse paths can offer higher reliability and tolerance to blockage, however, it also has a larger interference footprint and offers lower spatial reusability. Also, even though increasing the number of APs involved in a joint transmission can increase the robustness and RSS, more paths require the receiver to operate using wider beamwidths (discussed in Section 3), which in turn reduces the RSS after a certain extent. Since both reliability and spatial reusability directly impact network throughput, mmChoir uses the product of normalized reliability score and normalized spatial reuse score, and schedules the link transmissions on paths with high product score while meeting the interference constraints. The reliability scores are recalculated after every time slot based on the revised blockage probability values derived from observed blockages and resultant packet losses.

Our scheduling algorithm is shown in Algorithm 1. The scheduler runs at the controller which has the input information about the set of transmission requests including clients and data rate in a FIFO manner, the set of paths and their corresponding scores and updated blockage probabilities. The data rate can be translated to the RSS using the 802.11ad MCS table [7]. The scheduler tries to fit transmission requests in a given time slot greedily while satisfying RSS and interference constraints. It outputs the AP(s) (multiple in case of JT) and corresponding paths to be used to satisfy the requests. For each request, the scheduler first searches for the subset of paths that can satisfy the RSS (Line 6). For the candidate paths that can satisfy the request and do not interfere with other already scheduled paths in the slot (Line 7), the product of reliability and spatial reuses scores(Line 8) are compared. The scheduler uses a simple heuristic whereby the path with the maximum product is chosen to allow higher reliability and spatial reuse (Line 9). The output of the scheduler is a set of links which could be scheduled concurrently in one time slot. Once the links are scheduled for transmission (Line 17), the scheduler monitors the fraction of frames that were lost due to blockages, and uses that to update the blockage probability of each of the paths (Line 18). These updated blockage probabilities will be then used to calculate new reliability score for those paths before scheduling the next slot. This way, empirical observations are used to provide feedback to the scheduler allowing it to consider up-to-date blockage conditions in scheduling.

The size of the scheduling problem is $\sum_{i=1}^{|T|} \binom{|T|}{i} (|S|/n)^i$ where n is the number of clients and $|S|/n$ is the average number of available paths to a client from all APs within its range. We improve the running time of the algorithm by imposing two conditions. First,

Algorithm 1: mmChoir Scheduling Algorithm

Input: (i) FIFO backlogged queue T of active transmission requests $t_j = \{Rx_j, rss_j\}$ where Rx_j and rss_j are the requesting client and required RSS of the request; (ii) Path set S including individual and joint transmissions along with their estimated RSS, initial reliability score δ and spatial reuse score β for all $s_i \in S$; (iii) Conflict matrix C

Output: Transmission schedule L for each time slot where $L = \{l_1, l_2, \cdots, l_H\}$ is a set of concurrently scheduled transmissions and $l_h = \{t_h, s_h\}$ represents that path s_h is scheduled to transmit t_h

```
1  while T ≠ ∅ do
2      L ⟵ ∅
3      for each t_j ∈ T do
4          for each s_i ∈ {S | s_i → Rx_i = t_j → Rx_j} do
5              s_best ⟵ ∅
6              if s_i → rss_i ≥ t_j → rss_j then // Find eligible
                   paths
7                  if C(s_i, L → s_h) = 0 then // Interference
                       check
8                      Calculate δ(s_i) based on P_b(s_i)(Equ.4)
                         and β(s_i) using C
9                      if δ(s_i) × β(s_i) > δ(s_best) × β(s_best)
                         then // Find the path with the
                         highest product
10                         s_best ⟵ s_i
11                     end if
12                 end if
13             end if
14         end for
15         l_h ⟵ {t_j, s_best}; L ⟵ L ∪ l_h; T ⟵ T − {t_j}
16     end for
17     Schedule L for transmission
       // Observe blockages during transmission and
          update blockage probability
18     Update P_b(s_h) for all l_h → s_h ∈ L
19 end while
```

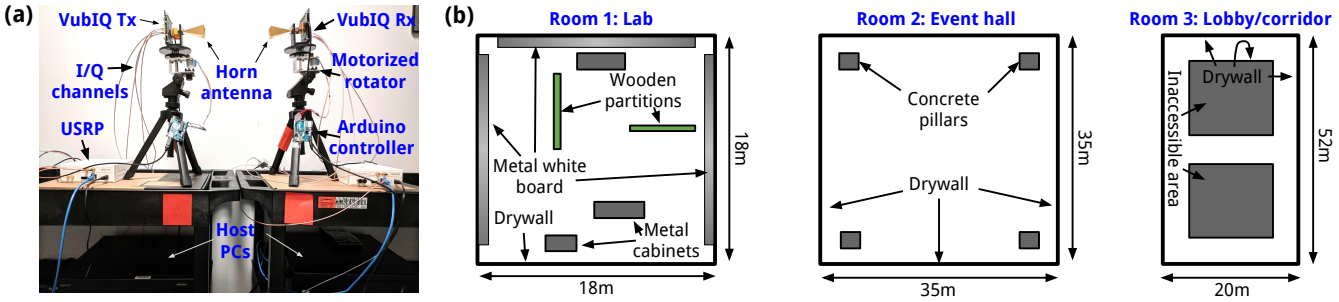

Figure 8: (a) Our 60 GHz software radio testbed composed of USRP, VubIQ 60 GHz RF frontend, Arduino-powered motorized rotator and horn antenna (b) Three rooms used in reflection profiling and simulations

given that no two requests of a client can be scheduled in one slot (receive conflict), we only consider first b requests of each client while scheduling. Assuming $n \times b \ll |T|$ in practice, this reduces the size to $\sum_{i=1}^{nb} \binom{nb}{i} (|S|/n)^i$. Second, the algorithm uses the transmit conflict as an early termination condition where maximum number of links scheduled in a slot cannot exceed m (total number of APs). With these two conditions, the running time of the scheduling algorithm is $(b-1)(n-1)(|S|/n) + n(n-1)(|S|/n)$, where $n(n-1)(|S|/n)$ is the worst case running time of fitting n clients together in one time slot and $(b-1)(n-1)(|S|/n)$ is the worst case running time of checking receive conflict for the queue of nb requests. Hence, the complexity is bounded by $O((b+n-1)|S|)$, and as noted before, $|S|$ is likely to small in practice due to mmWave channel sparsity.

6 EVALUATION

6.1 Experiment Setup

Testbed: Currently, there exists no commercially available 60 GHz transceiver system that allows reconfigurable beamforming. Fig. 8a shows our 60 GHz transmitter and receiver testbed. Both the transmitter and receiver uses a software radio (USRP N210 [21]) as the baseband signal generator and processor. The USRP is connected to VubIQ 60 GHz transmitter/receiver development platform [22] providing 60 GHz RF frontend. The frontend includes a horn antenna (12° half power beamwidth). As shown in Fig. 8a, the RF front-end module and the horn antenna are mounted on a mechanical rotator (tripod mounted on an assembly of motor, gears and shaft) which is controlled through an Arduino Uno. The host computer connects to the Arduino and USRP for control. The host computers are connected to the transmitter and receiver by using Ethernet. The transmitter USRP generates a 20 MHz baseband signal that is input to the VubIQ transmitter module. On the receiver side, the down converted signal is used by the USRP to calculate RSS.

Trace-driven Simulation Procedure: We evaluate mmChoir using trace-driven simulation by combining our 60 GHz testbed experiments and simulations. First, we choose three different types of rooms and carry out controlled experiments using our 60 GHz testbed. The objective of these experiments is to determine the indoor reflection profiles of these rooms. The profiles are then input to our simulator which uses ray tracing to simulate realistic propagation channels based on object reflectivity values, room layout, etc. The simulator also uses phased antenna array and codebook-based antenna patterns along with sidelobes for beamforming and interference estimation. Varying levels of dynamic human blockages are simulated along with stationary room blockages.

(1) Room Reflection Profiling: We consider three different rooms shown in Fig. 8(b) for our evaluation. The blockage and reflection characteristics of the three rooms are provided in Table 1. We carefully choose these three rooms as they are considerably different in terms of their size, layout related blockages and amount of reflections from ambient objects. Room 1 is a university laboratory which has relatively smaller area with moderate level of blockages related to layout (stationary objects like partitions, large major cabinets, etc.) and higher level of reflections. Room 2 is large event hall with few layout blockages and reflections. Room 3 is a building lobby/corridor that has high layout related blockages and reflections. We next describe the experiments to measure the indoor profile of the three rooms and also quantify the blockage and reflection as shown in Table 1.

Rooms	Amount of reflections	Layout blockages	Human blockages (simulated)
1	High	Moderate	Low, high
2	Low	Low	Low, high
3	High	High	Low, high

Table 1: Blockage and reflection characteristics of the three rooms shown in Fig. 8(b)

For a given indoor space, we first use our 60 GHz transmitter and receiver endpoints to profile its mmWave blockages and reflections using pilot measurements. It is known from prior research [19, 25] that different indoor objects, materials and surfaces reflect the incident mmWave signals differently. Specifically, the power of reflected signal depends on a variety of factors including the thickness of reflective source, signal incident angle and material's permittivity. The reflection loss $L_R = \frac{P_O}{P_I} = \Gamma^2$ where P_O and P_I are the values of power of reflected (after reflection) and incident (before reflection) signal respectively, and Γ is the reflection coefficient. The reflection coefficient can be calculated as [12]

$$\Gamma = \frac{1 - e^{-j2\kappa}}{1 - \Gamma_i'^2 e^{-j2\kappa}} \Gamma_i', \quad \text{for } i = \{\perp, \parallel\} \tag{5}$$

where $\delta = \frac{2\pi l}{\lambda} \sqrt{\epsilon_r - \sin^2\theta}$ and l indicates the thickness of the reflecting material, λ denotes the signal wavelength, θ is the signal

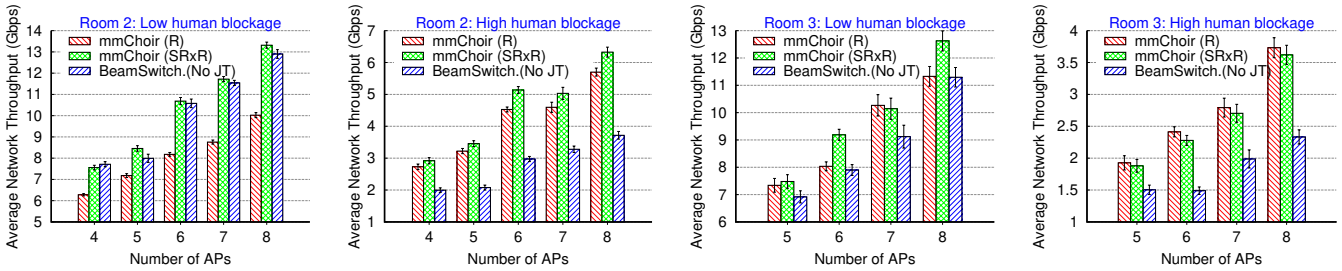

Figure 9: mmChoir (SRxR) uses fewer joint transmissions in lower blockage scenario and adaptively increases the joint transmissions in case of higher number of blockages to increase reliability and network capacity

incident angle, ϵ_r is the relative permittivity of the object. $\Gamma'_{\perp}$ and $\Gamma'_{\parallel}$ are the Frensel's reflection coefficients when the electric field is perpendicular and parallel to the incident plane.

For each of the rooms, we use 4 pairs of Tx-Rx locations and perform pilot RSS measurements. For each pair of locations, the Tx rotates 360° with angular steps of 12°, and Rx rotates 360° for each Tx angular step. We record $< \sigma_T, \sigma_R, RSS >$ where σ_T and σ_R are angles of transmission and reception, and use it to identify major ambient reflectors in the room. Our 4 pairs of pilot measurements result in 4 different $< \sigma_T, \sigma_R, RSS >$ tuples for each reflector. They are used to estimate the object permittivity of the reflector using Equ. 5. The reflection loss is calculated based on the transmit and receive side path loss values.

(2) Ray Tracing: The permittivity values for each point on the contour of the room surface and objects along with the actual room layout are now input to the simulator. The simulator uses a ray tracing model for mmWave propagation [16] to simulate channel propagation including reflections. We assume that each AP and client is equipped with 32 element antenna array (similar to QCA9500 [11]). Our simulator uses a multi-level codebook generated by MATLAB Phased Antenna Array toolbox and integrates it with the ray tracing propagation model to simulate beamforming including MIDC.

(3) Human Blockages: Apart from the stationary blockages of the room layout, we simulate random *dynamic human blockages* to evaluate the effectiveness of mmChoir in presence of human mobility and self-body blockage events. We model the dynamic human blockage probabilities of a link as a function of the beamwidth of the link's transmitter and receiver. This is based on the prior research [5, 19, 26] which shows that wider beamwidths are less prone to human blockages and dilation can be used as a mitigation technique. The blockage probability of ω degree pattern is represented as $p_\omega = \eta \times \frac{1}{\mu} e^{\frac{-\omega}{\mu}}$ where μ is the mean beamwidth of all patterns in the multi-level codebook and η is tunable parameter. Hence, the blockage probability of a link with ω_t degree transmitter pattern and ω_r degree receiver pattern can be calculated as $P_b(s_i) = p_{\omega_t} \times p_{\omega_r}$. We set η to 25 and 45 to simulate two levels (low and high) of human blockages (Table 1). The blockage events affect the links scheduled for transmission, which is then used to update the blockage probabilities as described in Algorithm 1.

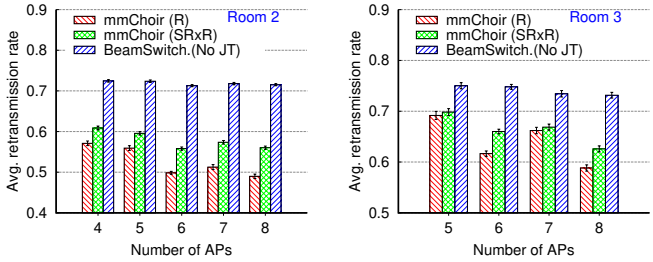

Figure 10: mmChoir intelligently chooses joint transmissions especially in moderate to high blockages, resulting in lower retransmission rate

6.2 Numerical Results

Using the trace-driven simulations, we compare the performance of three different schemes - **(1) mmChoir (SRxR)** which refers to mmChoir's scheduling algorithm where the product of reliability and spatial reuse scores is used to select paths and schedule links, **(2) mmChoir (R)** in which the scheduler only uses reliability score to path selection, resulting in a bias towards aggressively selecting more JTs (lesser spatial reuse) for improved robustness, and **(3) BeamSwitching (No JT)** which does not utilize joint transmissions but instead when a link faces blockage on a chosen path, it uses an alternate path (beamswitching) in the subsequent time-slot to retransmit the data. We assume that blockage detection and beamswitching can be accomplished in one time-slot (few milliseconds as shown in [19, 23]), so an alternate path can be chosen when the link is scheduled again for transmission. We vary the number of APs (by increasing it from the minimum number of APs needed for coverage) and number of clients (from 5 to 25) in all three rooms. The APs are uniformly deployed in each room while the clients are randomly placed. For each combination, the simulations are repeated 50 times and 90% confidence intervals are calculated.

Network Throughput: Figs. 9 and 10 show the average network throughput and retransmission rate for Room-2 and Room-3 respectively under low and high human blockages. We vary the number of APs and show the results for 25 clients. In case of a blockage, the packets sent during the service period on a transmission path that was blocked are retransmitted and rescheduled in subsequent slots until successfully delivered. In this case, the retransmission rate is calculated as the fraction of service periods

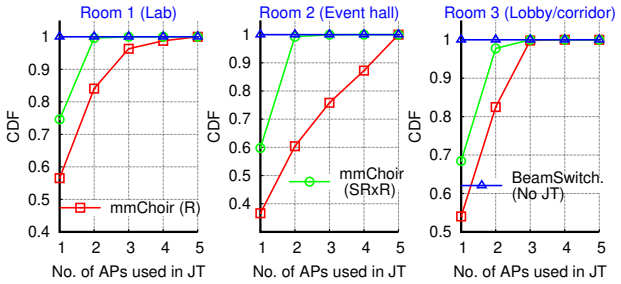

Figure 11: mmChoir(SRxR) utilizes fewer than 3 APs for a transmission in most cases depending on the level of blockages

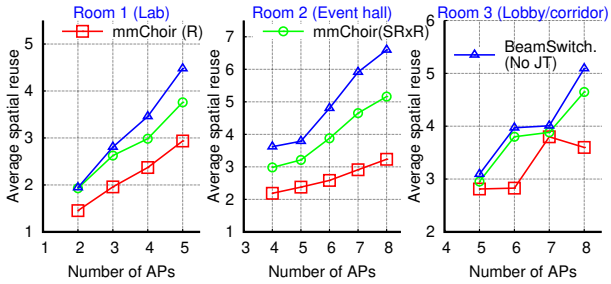

Figure 12: mmChoir(SRxR) achieves higher spatial reuse even in presence of joint transmissions due to its interference aware scheduling

that are required to be retransmitted. The network throughput is calculated based on the RSS of the scheduled links of the satisfied transmission requests and corresponding data rate from 802.11ad MCS table [7]. We observe that under various levels of human blockages, mmChoir outperforms the beamswitching scheme. This is because mmChoir can proactively provision for reliable paths to combat blockages while beamswitching is primarily reactive in nature.

Under low human blockages (Fig. 9), mmChoir(SRxR) achieves higher throughput compared to mmChoir(R) and BeamSwitching schemes. mmChoir(R) aggressively utilizes joint transmissions and gets penalized in terms of achievable spatial reuse, resulting in lower throughput. On the other hand, BeamSwitching often poorly reacts to the blockages compared to mmChoir(SRxR) which balances the spatial reuse and reliability by using fewer joint transmissions only as needed. In case of high human blockages (Fig. 9), mmChoir schemes based on joint transmissions clearly outperform the beamswitching scheme (71% and 49% higher throughput in Room 2 and 3 respectively). Since Room 3 has more stationary blockages (different from Room 2 which has larger open space), both mmChoir schemes achieve comparable throughput even in the low human blockage scenario. As shown in Fig. 10, retransmission rate decreases with more APs in case of mmChoir due to more opportunities for JT compared to the beamswitching scheme which cannot make use of additional resources. In conclusion, mmChoir(SRxR) adaptively adjusts the number of joint transmissions used to improve the reliability while maintaining high spatial reuse for both stationary layout blockages and dynamic human blockages. Across all three rooms, mmChoir(SRxR) achieves on an average 58.35% increase in network throughput and 14.54% decrease in retransmission rate under high human blockages.

Number of APs in JTs and Spatial Reuse: Fig. 11 shows the CDF of number of APs used by the three schemes under human blockage scenarios. We observe that mmChoir(SRxR) utilizes 1 AP or JT with 2 APs majority of the times. In Room 3 which provides fewer opportunities for the APs to do joint transmissions due to its stationary blockages, mmChoir(SRxR) involves more APs in joint transmissions to improve its reliability, while in Rooms 1 and 2, it balances individual transmissions and joint transmissions depending on the level of blockages. Fig. 12 shows the average spatial reuse in the three rooms. As expected, increasing the number of APs increases the spatial reuse. Given BeamSwitching (No JT) does not use joint transmissions, it achieves the highest spatial reuse. mmChoir (R) yields the lowest spatial reuse due to increased use of joint transmissions while mmChoir (SRxR), achieves a spatial reuse closer to that of BeamSwitching(No JT) especially in Rooms 1 and 2 due to its adaptive use of joint transmissions. In Room 3, all three schemes achieve lower spatial reuse mostly due to the layout related blockages. Even in such a scenario, mmChoir(SRxR) achieves a spatial reuse closer to that of BeamSwitching(No JT). This way, mmChoir(SRxR) can intelligently find the amount of JTs needed based on the blockages and the number of APs to use in the JTs to balance the reliability and spatial reuse.

7 RELATED WORK

60 GHz channel propagation has been studied by a number researchers in recent years. Authors in [24] performed early research in profiling 60 GHz indoor channels, path loss, reflections, power delay and power angular profiles. Recently, [19] performed detailed link-layer characterization for indoor spaces, while [27] profiled the mmWave links in outdoor settings. Blockage resistance in 60 GHz networks has been studied actively in recent years. Beam dilation and steering have been identified as potential solutions for blockage mitigation in early work [19]. Authors in [5] proposed the use of probing frames to identify blockages before sending the data and used alternate paths to circumvent blockages. Authors in [26] used beam dilation and beam steering but relied on sensor hints from a client device to switch the beams. It was identified in [20] that correlation between the signal strength of different sectors can be used to determine which fail-over paths can be used in presence of blockage. As noted before, these approaches are primarily reactive in nature. Authors in [23] proposed a self-body blockage mitigation technique where the mobile device's pose is detected using the motion sensors and based on the angle and orientation, an appropriate AP can transfer data to the client. mmChoir does not have to rely on motion sensors which are often unavailable or erroneous. Instead, our approach carefully determines when a JT might be necessary and exploits this information to proactive choose which APs can transfer data to the client. Other research [18] use out-band measurements from 2.4/5 GHz WiFi to determine mobility/blockage of clients and to guide the beam steering process of 60 GHz links. In comparison, mmChoir is designed to operate purely using 60 GHz beamforming information.

CoMP and joint transmissions have been investigated actively in cellular networks [3] for increasing the signal strength for edge users. In comparison, we exploit the joint transmissions for blockage mitigation in this work. Directional antenna link scheduling and interference management have been studied in 2.4/5 GHz WiFi network. [8] proposed a greedy scheduler that for directional links in WLANs. However, the solution does not consider 60 GHz propagation and phased array characteristics.

8 CONCLUSIONS AND FUTURE WORK

In this paper, we presented a joint transmission strategy for 60 GHz WLANs where multiple APs can jointly transmit to a client. The joint transmissions provide added robustness against blockages. We propose a reliability metric based on angular spread and a novel interference estimation model to estimate spatial reusability. Our mmChoir scheduler jointly considers the reliability and spatial reuse scores of transmissions, and adapts to varying levels of blockages. mmChoir is evaluated in three different types of rooms using testbed experiments and simulation. We find that it can outperform the existing scheme that does not use joint transmissions in terms of achievable network throughput and reliability. As part of future work, we plan to model and assess the overhead of coordination for a enterprise-grade WLANs. Such WLAN APs are likely to be deployed on ceiling, requiring 3D beamforming. Such beamforming can change the interference footprint and mmChoir needs to be adapted to include it. Lastly, we plan to incorporate more realistic human mobility model and resultant blockages in our system.

ACKNOWLEDGMENTS

We would like to thank the anonymous reviewers for their valuable comments and feedback. This research is supported by NSF grant CNS-1730083.

REFERENCES

[1] Mansoor Alicherry, Randeep Bhatia, and Li (Erran) Li. 2005. Joint Channel Assignment and Routing for Throughput Optimization in Multi-radio Wireless Mesh Networks. In *Proceedings of the 11th Annual International Conference on Mobile Computing and Networking (MobiCom '05)*. ACM, New York, NY, USA, 58–72. https://doi.org/10.1145/1080829.1080836

[2] Gurashish Brar, Douglas M. Blough, and Paolo Santi. 2006. Computationally Efficient Scheduling with the Physical Interference Model for Throughput Improvement in Wireless Mesh Networks. In *Proceedings of the 12th Annual International Conference on Mobile Computing and Networking (MobiCom '06)*. ACM, New York, NY, USA, 2–13. https://doi.org/10.1145/1161089.1161092

[3] A. Davydov, G. Morozov, I. Bolotin, and A. Papathanassiou. 2013. Evaluation of Joint Transmission CoMP in C-RAN based LTE-A HetNets with large coordination areas. In *2013 IEEE Globecom Workshops (GC Wkshps)*. 801–806. https://doi.org/10.1109/GLOCOMW.2013.6825087

[4] P. Gupta and P. R. Kumar. 2000. The capacity of wireless networks. *IEEE Transactions on Information Theory* 46, 2 (Mar 2000), 388–404. https://doi.org/10.1109/18.825799

[5] Muhammad Kumail Haider and Edward W. Knightly. 2016. Mobility Resilience and Overhead Constrained Adaptation in Directional 60 GHz WLANs: Protocol Design and System Implementation. In *Proceedings of the 17th ACM International Symposium on Mobile Ad Hoc Networking and Computing (MobiHoc '16)*. ACM, New York, NY, USA, 61–70. https://doi.org/10.1145/2942358.2942380

[6] IEEE 802.11ay: Enhanced Throughput for Operation in License-Exempt Bands above 45 GHz. 2016. *http://www.ieee802.org/11/Reports/tgay_update.htm*.

[7] IEEE P802.11adTM/D4.0. 2012. Part 11: Wireless LAN Medium Access Control (MAC) and Physical Layer (PHY) Specifications Amendment 3: Enhancements for Very High Throughput in the 60 GHz Band, IEEE Computer Society. *IEEE Computer Society* (July 2012).

[8] Xi Liu, Anmol Sheth, Michael Kaminsky, Konstantina Papagiannaki, Srinivasan Seshan, and Peter Steenkiste. 2009. DIRC: Increasing Indoor Wireless Capacity Using Directional Antennas *(SIGCOMM '09)*. ACM, New York, NY, USA, 171–182.

[9] D. J. Love and R. W. Heath. 2003. Equal gain transmission in multiple-input multiple-output wireless systems. *IEEE Transactions on Communications* 51, 7 (July 2003), 1102–1110. https://doi.org/10.1109/TCOMM.2003.814195

[10] G. Nigam, P. Minero, and M. Haenggi. 2014. Coordinated Multipoint Joint Transmission in Heterogeneous Networks. *IEEE Transactions on Communications* 62, 11 (Nov 2014), 4134–4146. https://doi.org/10.1109/TCOMM.2014.2363660

[11] Qualcomm QCA9500. 2017. *https://www.qualcomm.com/products/qca9500*.

[12] Theodore S Rappaport et al. 1996. *Wireless communications: principles and practice*. Vol. 2. prentice hall PTR New Jersey.

[13] T. S. Rappaport, S. Sun, R. Mayzus, H. Zhao, Y. Azar, K. Wang, G. N. Wong, J. K. Schulz, M. Samimi, and F. Gutierrez. 2013. Millimeter Wave Mobile Communications for 5G Cellular: It Will Work! *IEEE Access* 1 (2013), 335–349. https://doi.org/10.1109/ACCESS.2013.2260813

[14] Shravan Rayanchu, Vivek Shrivastava, Suman Banerjee, and Ranveer Chandra. 2011. FLUID: Improving Throughputs in Enterprise Wireless Lans Through Flexible Channelization. In *Proceedings of the 17th Annual International Conference on Mobile Computing and Networking (MobiCom '11)*. ACM, New York, NY, USA, 1–12. https://doi.org/10.1145/2030613.2030615

[15] Swetank Kumar Saha, Yasaman Ghasempour, Muhammad Kumail Haider, Tariq Siddiqui, Paulo De Melo, Neerad Somanchi, Luke Zakrajsek, Arjun Singh, Owen Torres, Daniel Uvaydov, Josep Miquel Jornet, Edward Knightly, Dimitrios Koutsonikolas, Dimitris Pados, and Zhi Sun. 2017. X60: A Programmable Testbed for Wideband 60 GHz WLANs with Phased Arrays. In *Proceedings of the 11th Workshop on Wireless Network Testbeds, Experimental Evaluation & CHaracterization (WiNTECH '17)*. ACM, New York, NY, USA, 75–82. https://doi.org/10.1145/3131473.3131479

[16] D. Steinmetzer, J. Classen, and M. Hollick. 2016. mmTrace: Modeling millimeter-wave indoor propagation with image-based ray-tracing. In *2016 IEEE Conference on Computer Communications Workshops (INFOCOM WKSHPS)*. 429–434. https://doi.org/10.1109/INFCOMW.2016.7562115

[17] Daniel Steinmetzer, Daniel Wegemer, Matthias Schulz, Joerg Widmer, and Matthias Hollick. 2017. Compressive Millimeter-Wave Sector Selection in Off-the-Shelf IEEE 802.11ad Devices. In *Proceedings of the 13th International Conference on Emerging Networking EXperiments and Technologies (CoNEXT '17)*. ACM, New York, NY, USA, 414–425. https://doi.org/10.1145/3143361.3143384

[18] Sanjib Sur, Ioannis Pefkianakis, Xinyu Zhang, and Kyu-Han Kim. 2017. WiFi-Assisted 60 GHz Wireless Networks. In *Proceedings of the 23rd Annual International Conference on Mobile Computing and Networking (MobiCom '17)*. ACM, New York, NY, USA, 28–41. https://doi.org/10.1145/3117811.3117817

[19] Sanjib Sur, Vignesh Venkateswaran, Xinyu Zhang, and Parmesh Ramanathan. 2015. 60 GHz Indoor Networking Through Flexible Beams: A Link-Level Profiling. In *Proceedings of the 2015 ACM SIGMETRICS International Conference on Measurement and Modeling of Computer Systems (SIGMETRICS '15)*. ACM, New York, NY, USA, 71–84. https://doi.org/10.1145/2745844.2745858

[20] Sanjib Sur, Xinyu Zhang, Parmesh Ramanathan, and Ranveer Chandra. 2016. BeamSpy: Enabling Robust 60 GHz Links Under Blockage. In *Proceedings of the 13th Usenix Conference on Networked Systems Design and Implementation (NSDI'16)*. USENIX Association, Berkeley, CA, USA, 193–206. http://dl.acm.org/citation.cfm?id=2930611.2930625

[21] Ettus Research USRP N210. 2017. *https://www.ettus.com/product/details/N210-KIT*.

[22] Vubiq, Irvine, CA, USA. [n. d.]. *60 GHz Systems and Modules*. https://www.pasternack.com/60-ghz-systems-and-modules-category.aspx

[23] Teng Wei and Xinyu Zhang. 2017. Pose Information Assisted 60 GHz Networks: Towards Seamless Coverage and Mobility Support. In *Proceedings of the 23rd Annual International Conference on Mobile Computing and Networking (MobiCom '17)*. ACM, New York, NY, USA, 42–55. https://doi.org/10.1145/3117811.3117832

[24] Hao Xu, V. Kukshya, and T. S. Rappaport. 2002. Spatial and temporal characteristics of 60-GHz indoor channels. *IEEE Journal on Selected Areas in Communications* 20, 3 (Apr 2002), 620–630. https://doi.org/10.1109/49.995521

[25] Zhicheng Yang, Parth H. Pathak, Yunze Zeng, Xixi Liran, and Prasant Mohapatra. 2016. Monitoring Vital Signs Using Millimeter Wave. In *Proceedings of the 17th ACM International Symposium on Mobile Ad Hoc Networking and Computing (MobiHoc '16)*. ACM, New York, NY, USA, 211–220. https://doi.org/10.1145/2942358.2942381

[26] Z. Yang, P. H. Pathak, Y. Zeng, and P. Mohapatra. 2015. Sensor-Assisted Codebook-Based Beamforming for Mobility Management in 60 GHz WLANs. In *Mobile Ad Hoc and Sensor Systems (MASS), 2015 IEEE 12th International Conference on*. 333–341. https://doi.org/10.1109/MASS.2015.58

[27] Yibo Zhu, Zengbin Zhang, Zhinus Marzi, Chris Nelson, Upamanyu Madhow, Ben Y. Zhao, and Haitao Zheng. 2014. Demystifying 60GHz Outdoor Picocells. In *Proceedings of the 20th Annual International Conference on Mobile Computing and Networking (MobiCom '14)*. ACM, New York, NY, USA, 5–16. https://doi.org/10.1145/2639108.2639121